Proceedings of the 2003 IEEE International Frequency Control Symposium and PDA Exhibition
Jointly with the 17th European Frequency and Time Forum

METROLOGICAL ASPECTS OF THE ON-METAS CONTINUOUS FOUNTAIN STANDARD

A. Joyet[1], N. Castagna[1], P. Thomann[1], G. Dudle[2], C. Mandache[3], T. Acsente[3]

[1]Observatoire Cantonal (ON), CH-2000 Neuchâtel, Switzerland
[2]Swiss Federal Office of Metrology and Accreditation (METAS), CH-3003 Bern-Wabern, Switzerland
[3]National Institute for the Physics of Laser, Plasma and Radiation (INFLPR), Bucharest-Magurele

Abstract – **We report on the preliminary evaluation of two metrological aspects specific to a primary standard based on a continuous fountain of laser-cooled Cs atoms. This type of standards takes advantage of the reduced density of the cold atoms beam which should result in a negligible collisional frequency shift. We describe a new theoretical evaluation of the average atomic density; in present flux condition, the calculation gives an average density corresponding to a shift of $0.7 \cdot 10^{-17}$. With the present atomic source intensity and in the limit of zero transverse temperature, the estimated collisional shift would be $<10^{-16}$ for a short-term stability of $1 \cdot 10^{-13} \tau^{-1/2}$.**
On the other side, the continuous operation of the fountain requires to separate the light emitted by the source of cold atoms from the continuous atomic beam to be interrogated. Without light-trap, in addition to the expected light shift, the measured Ramsey fringes show a reduction of the contrast which can be reproduced by a model of loss of population of the F=4, m_F=0 hyperfine level due to optical pumping by the fluorescence light from the source. The model also reproduces the asymmetric damping of the measured Rabi oscillations.
The present state of the accuracy budget is also given taking into account measured stray light intensities at cavity level with and without light trap.
Keywords – **Continuous atomic fountain, atomic frequency standard, light shift.**

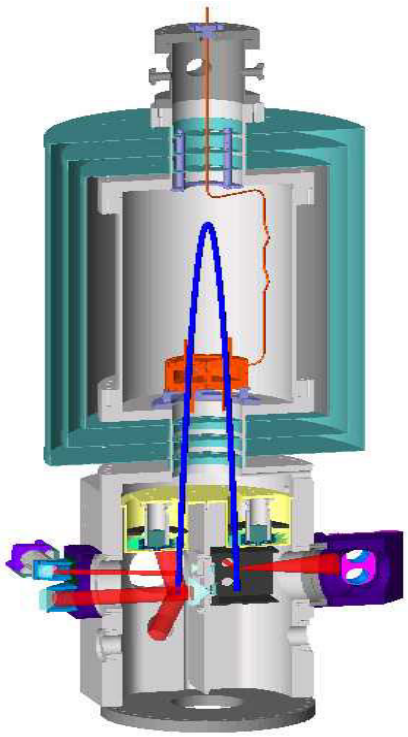

Fig.1 Schematic view of the fountain resonator. The height of the drawn parabola is 75 cm.

I. INTRODUCTION

Most prototypes of cesium fountain frequency standards rely on a pulsed mode of operation [1]. Atomic fountains have already shown their potentiality to improve significantly both the short-term stability and the accuracy of the Cs standards; however, their operation in a pulsed mode may introduce difficulties in achieving the ultimate short-term stability and accuracy that the use of slow atoms allow in principle. The best accuracy in Cs fountains is achieved with moderate atomic densities to limit the contribution of the collisional shift, which is proportional to the cold cloud density. The short-term stability, however, improves as the square-root of the number of atoms probed in each cycle, and its optimisation would require as high an average atomic flux as possible. Moreover, pulsed operation of passive frequency standards provides an undesirable aliasing mechanism through which the phase noise of the interrogation oscillator may severely limit the achievable short-term stability [2], [3].

The continuous beam approach [4], [5] provides a simple way of reducing by about two orders of magnitude both the collisional shift and the aliasing effects tied to pulsed operation, thus relaxing the compromise between accuracy (as potentially limited by the collisional shift) and stability. Fig.1 shows a cut through the continuous cesium fountain developed at the Observatoire cantonal of Neuchâtel (ON) in collaboration with the Swiss Federal Office of Metrology and Accreditation (METAS).
Details on the device itself have been published earlier [4].
This communication reports on the investigations of two aspects which are specific to the continuous fountain. First, in order to predict the collisional shift expected at a given flux and short-term-stability, we present a theoretical model that describes the evolution of the atomic density along the parabolic flight of cold beam[6].
Second, we discuss a model that describes perfectly the reduction of contrast of the Ramsey fringes which has been observed experimentally earlier[6]. The main ingredient for

this model is optical pumping in the microwave cavity due to unattenuated fluorescence from the source of cold atoms.
Third, we present some results on the estimated light shift due to the stray light, that confirm the predicted expectations[7], [8].
Finally, a summary of the partial accuracy budget of the standard is presented.

II. COLLISIONAL SHIFT IN A CONTINUOUS FOUNTAIN

Due to the fact that for the same average S/N ratio a continuous fountain works with a highly reduced atomic density with respect to a pulsed fountain, the collisional shift is believed to be negligible in the former case. Nevertheless, it is not sufficient to invoke the average argument, since the atomic density undergoes major changes along the trajectory of the cold atoms. Therefore it is necessary to evaluate the atomic density along the parabolic flight of the atoms.
The model presented here is based on the following assumptions:

1. Gaussian distribution of the longitudinal velocity of the beam with temperature T_l and an average initial velocity equal to 3.85 ms^{-1};
2. Gaussian distribution of the transverse velocity of the beam with isotropic temperature before transverse cooling, transverse temperature T_t thereafter and average transverse velocity equal to 11.2 $cm \cdot s^{-1}$;
3. The flux is conditioned by the passage through only three relevant diaphragms shown in bold in fig. 2 (access hole to the light trap, the two passages through the microwave cavity);
4. The beam evolution is considered as a path along the horizontal direction; this approach simplifies the problems of a simulation for a parabolic flight, especially around the apogee;
5. Gaussian distribution of the initial beam density.

The beam atomic density can be written as:

$$n(\vec{r},t) = n_z(t) \cdot n_S(\vec{r},t)$$

where $n_z(t)$ is the linear density due to the longitudinal movement and $n_S(\vec{r},t)$ is the surface density; the evolution of this one follows a gaussian law:

$$n_S(\vec{r},0) = n_{S0} \exp[-r^2 / R_0^2]$$

with

$$n_{S0} = 1/(\pi R_0^2)$$

where R_0 is the mean quadratic radius of the initial surface density and n_{S0} is the initial density value at the centre of the beam.

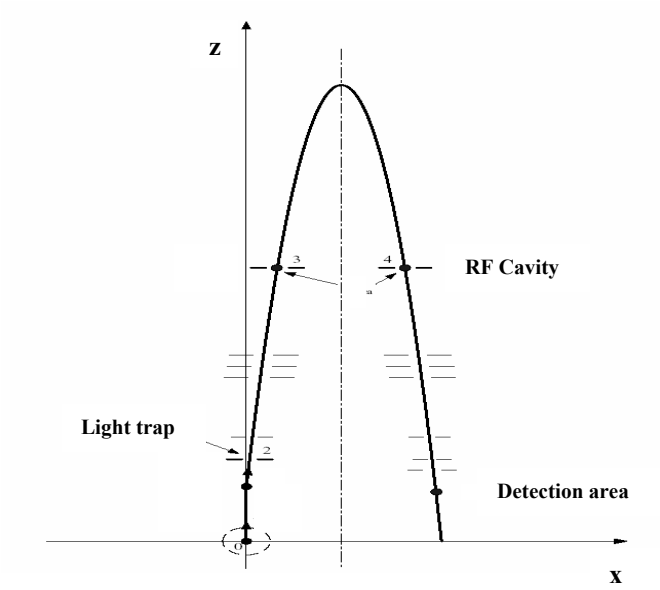

Fig. 2 Parabolic flight of the atomic beam with all the diaphragms present on the continuous fountain; the bold diaphragms are the ones considered in the analytical model.

Given a Gaussian distribution of the longitudinal and transverse velocity

$$\rho(v_t) = 1/(\pi v_{t_{rms}}^2) \exp[-v_t^2 / v_{t_{rms}}^2]$$
$$\rho(v_l) = 1/(\sqrt{2\pi} \cdot v_{l_{rms}}) \exp[-(v_l - \bar{v}_l)^2 / 2v_{l_{rms}}^2]$$

a Monte Carlo simulation yields a ratio between the detected and the initial flux. Fig.3 shows this ratio as a function of the mean launch velocity $\bar{v}_l$. Some experimental points are also reported in the same graph (circles); the agreement between experiment and the model validates the assumptions.

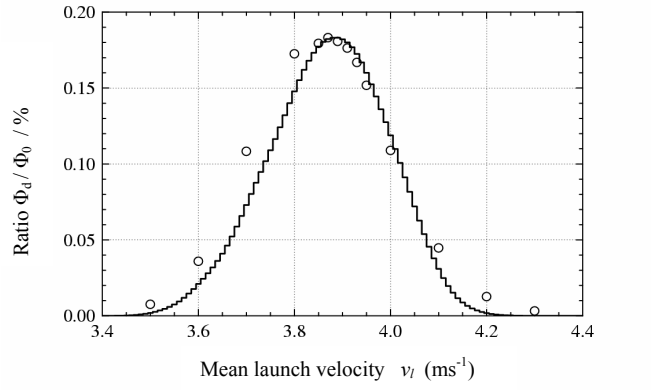

Fig. 3 Ratio between the detected and the initial flux as a function of the mean launch velocity; we consider a beam without transverse cooling and with the microwave cavity.

Using the beam geometry validated by the preceding simulation and results, we now calculate the average density $\bar{n}$ of the beam above the microwave cavity; to do this, we

have also to consider atoms which collide but are not necessarily detected or are not involved in the clock transition. The principle applied for this calculation is graphically represented in Fig.4; let us first describe the main steps of the calculation:

- The beam density after the passage through the RF cavity is considered constant (because its gaussian distribution is much wider than the dimension of the cavity cut-off tube)
- We calculate the average density at height z for a gaussian transverse velocity distribution along x axis with a fixed longitudinal velocity
- In order to consider the different distribution density for x values corresponding to the same fixed level z, we add these distributions (up and down beams)
- Sum over longitudinal velocity distribution
- We consider the truncation imposed by the diaphragms
- We calculate $\overline{n}$ in the volume swept by atoms that can reach the detection area only; $\overline{n}$ includes however all atoms in that volume, including those that will not reach the detector

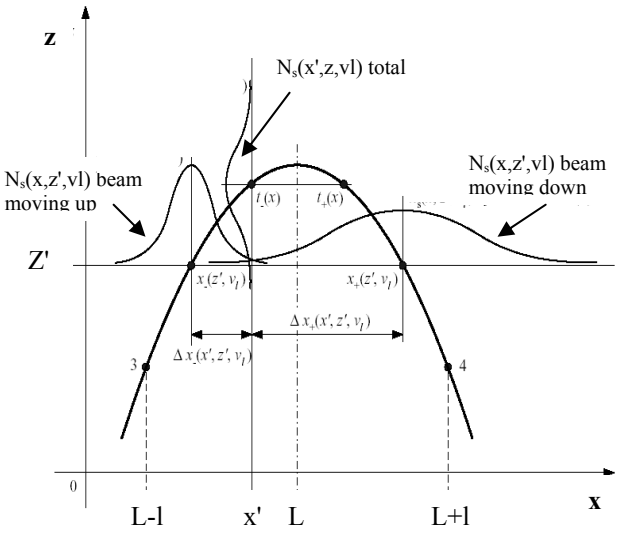

Fig. 4 Outline for the principle used to calculate the total surface density distribution of the beam $n_s(x,z,v_l)$; the distributions for a fixed abscissa x' and a fixed altitude z' are also shown. The graph is drawn for a monokinetic beam.

With the typical parameters of the continuous fountain that are reported in Tab.1 the result is:

$$\overline{n} \cong 0.65 \cdot n_0$$

where n_0 is the value of the density at the source. From experimental measurements we estimate that n_0 is equal to $1.3 \cdot 10^4$ at/cm^3.

The relative collisional frequency shift corresponding to a cold flux of atoms is given by [9]:

$$\Delta\nu / \nu = -0.8 \cdot 10^{-21} \overline{n}$$

Applying the average density obtained above, we expect a collisional shift smaller than $0.7 \cdot 10^{-17}$, a value that can safely be neglected. This value is in fact an upper limit because the constant that appears in the formula is obtained for an atomic beam colder than ours; if we increase the flux by cooling further the beam in the radial and longitudinal direction to a temperature near zero, the corresponding average density would increase by a factor of 9 leading to a relative shift of the order of 10^{-16} only; however, the expected gain of atomic flux is of the order of 5, leading to a short term stability of $1 \cdot 10^{-13}\ \tau^{-1/2}$, assuming the presently achieved atoms source flux.

Parameter	Symbol	Value
Longitudinal temperature	T_l	75 µK
Transverse temperature	T_t	5 µK
Distance source-parabole axis	L	43.6 mm
Semi-distance cavity holes	l	28 mm
Mean transit time	T	0.51 s
Mean launch velocity	v_l	3.85 m/s
Cavity holes diameter	d	9 mm

Tab. 1 Some typical parameters measured on the continuous fountain. The value of the longitudinal temperature is considered after the transverse cooling.

III. MODELLING OF OBSERVED LIGHT SHIFT AND OPTICAL PUMPING EFFECTS

We now consider the measured Ramsey fringes; Fig.5 shows the experimental result confronted to a simulation where a loss of population of the $|F=4,m_F=0>$ hyperfine level due to optical pumping is introduced; the optical pumping rate used in the simulation is deduced from the measured light shift value before the introduction of the light-trap, that is $1.4 \cdot 10^{-12}$. The experimental loss of fringe contrast is correctly accounted for by the model..

If we now consider the Rabi oscillations (see Fig.6), that are the variation of the maximum (Ω_0=0 Hz) and the minimum ((Ω_0=1 Hz) of the central fringe as a function of the microwave power, we note that the model does not match the experimental result: the loss of population of the $|F=4,m_F=0>$ hyperfine level is not enough to explain the experimental result which presents a positive slope superimposed with the damping of the Rabi oscillations.

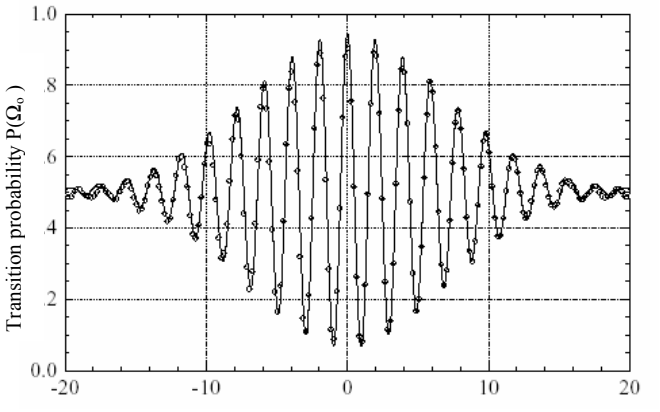

Fig. 5 Ramsey fringes. The white circles are the measured point and the continuous line is the theoretical result for a model that includes a loss of population of the level $|F=4,m_F=0>$ due to the Zeeman optical pumping.

Measured points and theoretical model become in good agreement if we add to the model the transverse distribution of the Rabi frequencies; indeed:

- The beam has a transverse dimension and a transverse temperature different from zero;
- The beam is not parallel to the *z* axis, consequently the magnetic field seen by the atoms is deformed.

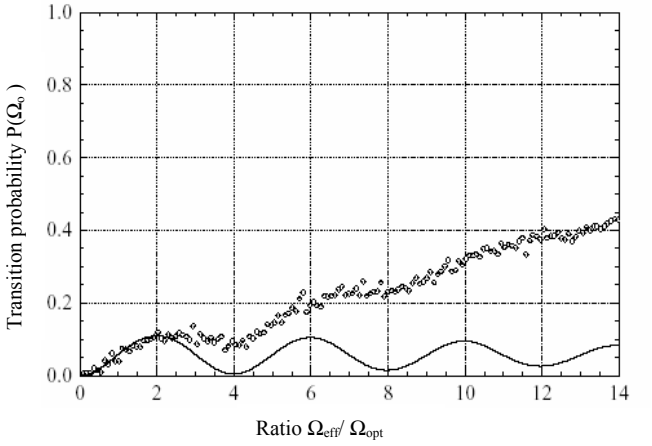

Fig. 6 Rabi oscillations (Ω_0=1 Hz, fringe minimum). The white circles are the measured point and the continuous line is the theoret at ical result for a model that includes a loss of population of the hyperfine level $|F=4,m_F=0>$ due to the Zeeman optical pumping.

Fig.7a (Ω_0=0 Hz) shows the experimental data and the model calculation including the Rabi distribution frequencies, which accounts well for the stepwise damping of the Rabi oscillations. Fig.7b (Ω_0=1 Hz) shows the same thing for the minimum of the central fringe; we can observe that now experimental data match well the model calculation.

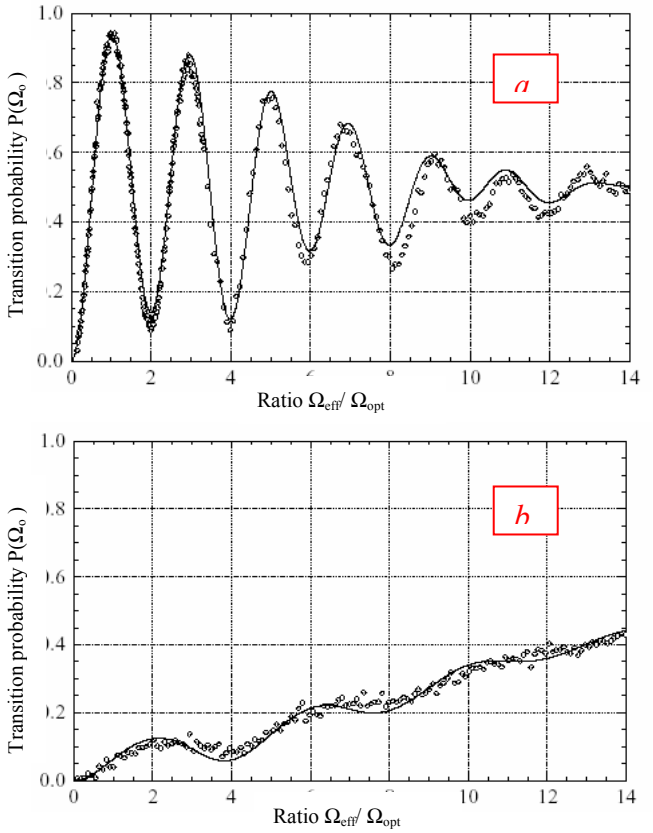

Fig. 7 Rabi oscillations. The white circles are the measured point and the continuous line is the theoretical result for a model that includes a loss of population and a Rabi frequencies distribution. graph (a) is relative to the maximum of the central fringe, graph (b) is relative to the minimum.

IV. LIGHT SHIFT REDUCTION

For an arbitrary light source spectrum given by g(δ/Γ), the relative light shift is:

$$\Delta\nu/\nu = 13.55\cdot10^{-6}\, I\cdot\int_{-\infty}^{+\infty} g(\delta/\Gamma)\,\frac{4\cdot\delta/\Gamma}{1+4(\delta/\Gamma)^2}\,d(\delta/\Gamma)$$

where $\Gamma=2\pi\cdot5.3$ MHz and $\delta=\omega-\omega_0+k\cdot v_r$; ω is the source frequency, ω_0 is the atomic resonance frequency and v_r is the relative velocity of the atoms at the source in comparison with the one at the Ramsey cavity level; the light intensity I is measured in $W\cdot m^{-2}$.

This expression has been calculated for the light shift of the $|F=4>$ level with $\omega_0=\omega_0(|F=4> \rightarrow |F'=5>$ transition). The function g(δ/Γ) is a Doppler broadened spectrum for the hot atoms fluorescence component, a Lorentz spectrum for the cold atoms fluorescence and a Delta of Dirac for the stray laser light.

A) No light-trap

We have calculated, in the geometry of the continuous fountain, the contribution to the total light shift of the light components emitted from the source; the result is a shift

equal to $-3\cdot10^{-13}$ produced from the hot atoms and a shift of $+1.6\cdot10^{-12}$ produced from the cold atoms; since the total measured light shift is $1.4\cdot10^{-12}$ we can conclude that the light shift is dominated by the fluorescence light due to the cold atoms component.

B) *With light trap*

We have measured that the introduction of the light-trap reduces the light intensity above the cavity by more than four orders of magnitude. On the other hand the stray laser light is completely under control after the introduction of graphite and Aquadag paint in strategic regions; its intensity has been measured with a photodetector fixed along the trajectory of the parabolic flight, 225 mm above the source, and the result is a contribution to the light shift in the order of 10^{-16}, which is clearly negligible.

We estimate indeed to have resolved any problem tied to the light shift that could prevent the desired accuracy. The fountain is now ready for evaluation with the light-trap.

IV. CONCLUSIONS

A model that describes perfectly the observed reduction of contrast of the Ramsey fringes has been developed.

On the other hand, we can affirm that any problem tied to the light shift is now well known and weighted.

We present in Tab 2 a partial state of the accuracy budget taking into account measured stray light intensities at cavity level.

Shift	Value	Uncertainty
Zeeman second order (*)	$2.44\ 10^{-14}$	$3\ 10^{-14}$
Light shift without trap (*)	$1.4\ 10^{-12}$	-
Light shift with trap (***)	$< 10^{-15}$	$< 10^{-14}$
Collisional shift (***)	$0.7\ 10^{-17}$	$< 10^{-14}$
End-to-End phase shift (**)	$< 5\ 10^{-14}$	$< 10^{-15}$
Distributed phase shift (**)	$4\ 10^{-17}$	$< 10^{-14}$

Tab.2 Present state of the accuracy budget given taking into account measured stray light intensities at cavity level.

ACKNOWLEDGMENT

We thank METAS, the State of Neuchâtel (NE) and the Swiss National Science Foundatation (SNSF) for their financial support.

REFERENCES

[1] A. Clairon, C. Salomon, S. Guellati and W.D. Phillips, "Ramsey resonance in a Zacharias fountain", *Europhys. Lett*., vol. 16, pp. 165-170, 1991.

[2] A. Joyet, G. Mileti, P. Thomann and G. Dudle, "Theoretical study of the Dick effect in a continuously operated Ramsey resonator", *IEEE Trans. Instr. Meas*., Vol. 50, No. 1, pp. 150-156, Feb. 2001.

[3] G.J. Dick, J.D. Prestage, C.A. GreenHall and L. Maleki, "Local oscillator induced degradation of medium-term stability in passive atomic frequency standard", in *Proc. 22nd PTTI Meet*., Redondo Beach, California, 1987, pp. 133-140.

[4] G. Dudle, G. Mileti, A. Joyet, E. Fretel, P. Berthoud and P. Thomann, "An alternative cold cesium frequency standard: the continuous fountain", *IEEE Transactions on Ultrasonics, Ferroelectrics and Frequency Control*, Vol. 47, No. 2, Mar. 2000, pp. 438-442.

[5] P. Berthoud, E. Fretel, and P. Thomann, "Bright, slow, and continuous beam of laser-cooled cesium atoms", *Physical Review A 60*, Dec. 1999, R4241-4244.

[6] A. Joyet, "Aspects métrologiques d'une fontaine continue à atoms froids", *PhD Thesis,* University of Neuchâtel, Switzerland, *2003*.

[7] A. Joyet, G. Mileti, P. Thomann and G. Dudle, "Continuous fountain CS standard: stability and accuracy issues", in *"Frequency standards and metrology", Proceedings of the 6th Symposium*, St. Andrews, Scotland, pp. 273-280, , World Scientific 2002, ISBN 981-02-4911-X.

[8] A.Joyet, G.Mileti, P.Thomann, G.Dudle, C.Mandache and T.Acsente, "Stability and Accuracy Results with the ON/METAS Continous Cesium Fountain", *CPEM*, Ottawa, Canada, 2002.

[9] S. Ghezali, Ph. Laurent, S.N. Lea and A. Clairon, "An experimental study of the spin-exchange frequency shift in a laser-cooled cesium fountain standard", *Europhys. Letters,*36(1): 25-30,1996.